Surface modifications at the oxide/water interface: implications for Cu binding, solution chemistry and chemical stability of iron oxide nanoparticles

Edwige Demangeat, Mathieu Pédrot, Aline Dia, Martine Bouhnik-Le Coz, Mélanie Davranche, Francisco Cabello-Hurtado

Surface modifications at the oxide/water interface: implications for Cu binding, solution chemistry and chemical stability of iron oxide nanoparticles

Edwige Demangeat[a], Mathieu Pédrot[a,*], Aline Dia[a], Martine Bouhnik-Le-Coz[a], Mélanie Davranche[a] and Francisco Cabello-Hurtado[b]

[a] Univ. Rennes, CNRS, Géosciences Rennes - UMR 6118, 35000 Rennes, France
[b] Univ. Rennes, CNRS, Ecobio - UMR 6553, 35000 Rennes, France

Abstract

The oxidation of magnetite into maghemite and its coating by natural organic constituents are common changes that affect the reactivity of iron oxide nanoparticles (IONP) in aqueous environments. Certain ubiquitous compounds such as humic acids (HA) and phosphatidylcholine (PC), displaying a high affinity for both copper (Cu) and IONP, could play a critical role in the interactions involved between both compounds. The adsorption of Cu onto four different IONP was studied: magnetite nanoparticles (magnNP), maghemite NP (maghNP), HA- and PC-coated magnetite NP (HA-magnNP and PC-magnNP, respectively). According to the results, the percentage of adsorbed Cu increases with increasing pH, irrespective of the IONP. Thus, protonation/deprotonation reactions are likely involved within Cu adsorption mechanism. Contrary to the other studied IONP, HA-magnNP favor Cu adsorption at most of the pH tested including acidic pH (pH = 3), suggesting that part of the active surface sites for Cu^{2+} were not grabbed by protons. The Freundlich adsorption isotherm of HA-magnNP provides the highest sorption constant K_F (bonding energy) and n value which supports a heterogeneous sorption process. The heterogeneous adsorption between HA-magnNP and Cu^{2+} can be explained by both the diversity of the binding sites HA procured and the formation of multidendate complexes between Cu^{2+} and some of the HA functional groups. Such favorable adsorption process was neither observed on PC-coated-magnNP nor on maghNP, whose behaviors were comparable to that of magnNP. On another hand, HA and PC coatings considerably reduced iron (Fe) dissolution from magnNP as compared with magnNP. It was suggested that HA and PC coatings either provided efficient shield against Fe leaching or fostered dissolved Fe re-adsorption onto the functional groups at the coated magnNP surfaces. Thus, this study can help to better understand

the complex interfacial reactions between cations-organic matter-colloidal surfaces which are relevant in environmental and agricultural contexts.

This work showed that magnetite NP properties can be affected by surface modifications, which drive NP chemical stability and Cu adsorption, thereby affecting the global water chemistry.

Keywords: *magnetite oxidation, surface coating, humic acid, phosphatidylcholine, copper adsorption, copper speciation*

* Corresponding author: mathieu.pedrot@univ-rennes1.fr Phone (+33)2 23 2360 83

Declarations of interest: none

1. Introduction

For almost two decades, engineered nanoparticles (NP), one of many nanomaterials, have been revolutionary tools to human kind. Due to their nano-scale size, NP displays a high surface to volume ratio which provides them with promising properties in many areas (Gupta and Gupta, 2005, Afkhami et al, 2010, Dabrowski et al., 2004). More specifically, engineered iron oxide NP (IONP) display high reactivity, magnetic properties and biocompatibility that allow their use in many technical applications. Examples of these uses range from medical therapies (Wu et al., 2015, Karimi et al., 2013), imaging and recording technologies to remediation methods and agricultural practices (Sabbatini et al., 2010, Khot et al., 2012). The application of iron nanoparticles (IONP) for soils and water remediation, in particular, has been explored for a few decades and several studies have highlighted the affinity of metals and metalloids for these objects (Wang et al., 2012, Ahmed et al., 2013, Pan et al., 2010).

Sorption reactions with both organic and inorganic compounds play a key role in the transport and fate of many trace elements in natural systems (Ye et al., 2017). Binding of metals on oxide minerals, in particular, involves predominantly electrostatic interaction (non-specific sorption) or chemical interaction (specific sorption) (Smith, 1999). According to Hu et al., (2006), metal ion sorption onto magnetite has been shown to involve both electrostatic attraction and ligand exchange at various pH conditions. In aqueous environments, IONP are amphoteric solids that become charged in response to the (de)protonation reactions of the Fe-OH surface sites (Pang et al., 2007). Consequently, dissolved cationic species are attracted to IONP at pH values higher than their pH_{zpc} (point of zero charge), where the surfaces of the IONP are

negatively charged. In fact, the mechanisms responsible for IONP and metal interactions are dependent upon several geochemical parameters such as pH, ionic strength, temperature and soil solution chemistry including the initial metal concentration and the adsorbent (IONP) concentration (Stumm, 1992; Smith, 1999). To take into account the role of these parameters and describe the resulting binding mechanisms of cations (or protons) onto oxide mineral surfaces, surface complexation models are implemented based on similar principles (sorption of ions occurs at specific coordination sites; sorption equations are described by mass law equations; sorption of ions control solid surface charge; electrostatic effects on ions binding are considered) (Smith, 1999).

The physico-chemical properties of IONP also do play a key role in cation adsorption processes (Parkinson, 2016). These intrinsic properties are likely modified when IONP are released in natural environments because of the numerous transformations that IONP undergo and the interactions that occur with natural constituents and living organisms (Joo and Zhao, 2017, Amde et al., 2017). Phase transformations, affecting the whole mineral structure, can stem from dissolution, precipitation, oxidation-reduction reactions, photochemical transformations or other internal structural changes (Tang and Lo, 2013, Löhr et al., 2017). In addition, co-precipitation, sorption and certain biotransformations can also affect the interactions occurring at the surfaces of the IONP and thus modify their reactivity as well as the behavior of some constituents, such as metal speciation (Nowack and Bucheli, 2007).

Once released into the ecosystems, IONP may be coated with organic substances due to the pervasiveness of these compounds in natural areas (Tang et al., 2014). As part of the dissolved organic matter, humic acids (HA), consist of a complex, heterogeneous arrangement of high- to low-molecular weight species exhibiting different water solubilities and reactivities. Hence, HA displays a high affinity for magnetite, and the adsorption of HA onto magnetite NP has been proven to largely impact the physicochemical properties of iron oxides such as their colloidal stability (Illés and Tombacz, 2006, Ghosh et al., 2011, Hadju et al., 2009, Grillo et al., 2015, Tombacz et al., 2013, Demangeat et al., 2018) and also, their interactions with soil solution species including several metals (Vindedahl et al., 2016, Davranche et al., 2013, Yu et al., 2018). Indeed, HA contain metal-binding functional groups (such as carboxylates, phenols, amines, thiols) with binding affinities and ligand densities that range several orders of magnitude. Phospholipids, another ubiquitous family of compounds, are also commonly found in natural

waters. Phosphatidylcholine (PC), in particular, is a major component of living organisms and it is largely employed in the agro-industry (Brown et al., 1999). Therefore, it is expected that phosphatidylcholine can cover the surfaces of the IONP in surface waters and possibly, interfere in the interactions between the metals and the IONP (Debnath et al., 2010). PC likely form lipid bilayers onto mineral surfaces in aqueous mediums because of their amphiphilic character and they can form various structures depending on the properties of these molecules (Mulder et al., 2006, Giri et al., 2005). Therefore, PC coating can impact the surface structure of the IONP and the ensuing interactions between the coated surface and metal ions mainly via electrostatic interactions (Solis-Calero et al., 2015). In addition to surface coatings, magnetite is also chemically unstable. The oxidation of magnetite NP into maghemite NP likely induces structural and chemical changes which are of great concern towards contaminant interactions, including metal adsorption (Frison et al., 2013, Gorski et al., 2010, Hu et al., 2005).

IONP interactions with metals are relevant towards many applications because of the ensuing environmental and societal impacts (Kah, 2015). Many studies have focused on the adsorption capacity between some IONP and certain metals with the aim to investigate the potential of some new depollution means or to precise the limits of such environmental applications. However, although the effects related to the properties of the medium are often investigated to decipher the adsorption process itself, their impacts on the behavior and fate of IONP are frequently neglected despite their relevance towards several other mechanisms (such as, NP dissolution, metal co-precipitation, etc.). Besides, much interest should be given to the interactions between IONP and copper (Cu) since these compounds are of increasing concern in various sectors whether it is for industrial, agricultural or environmental purposes (Li et al., 2016, Adrees et al., 2015). Significant quantities of iron (in the form of IONP) along with dissolved copper are released into the acidic waters coming from mining wastes and acid mine drainage (Mohan et al., 2006, Otero-Farina et al., 2015). Besides, the use of pesticides, fungicides, wastewater irrigation and other industrial effluents (related to petroleum refining, electroplating, foundries) also result in high concentrations of copper in soils and waters (Mohan et al., 2006; Adrees et al., 2015). In these mediums, toxic level of Cu most often hampers sustainable agriculture as well as food and health safety (Adrees et al., 2015). In this frame, several studies have shown the potential of IONP to remove Cu^{2+} from aqueous solutions as well as the effects of HA coating onto magnetite nanoparticles reactivity (Christl and Kretzschmar, 2001; Liu et al.,

2008). However, the impacts of IONP/Cu interactions on the nanoparticle stability and on the solution chemistry (especially Cu speciation) still raise a number of questions that are rarely tackled.

In the present study, the adsorption capacity of four different IONP was investigated using increasing amounts of Cu. The IONP included magnetite NP (magnNP), its oxidized form maghemite (maghNP), magnetite NP coated with humic acid (HA-magnNP) and magnetite NP coated with phosphatidylcholine (PC-magnNP). Thus, the scenario tested in this study is intended to: (i) identify the physico-chemical modifications induced by oxidation and by two different surface coatings on magnNP, (ii) decipher how these modifications are involved regards to magnNP chemical stability (dissolution rate), (iii) and how they can drive Cu adsorption at the surface of the IONP, and, (iv) provide insights into the relationships that possibly exist between IONP dissolution, IONP reactivity and their colloidal stability.

2. Materials and methods

2.1. IONP

2.1.1. Synthesis procedures

Magnetite (Fe_3O_4) NP were synthesized following the method of Khalafalla and Reimers (1980) and Massart (1981) using $FeCl_2.4H_2O$ and $FeCl_3.6H_2O$ salts.

Maghemite (γ-Fe_2O_3) NP were prepared based on the method of Zasonska et al. (2016), by oxidizing the magnetite nanoparticles.

Coatings of magnetite NP were performed using HA (Elliott Soil Humic Acid Standard IV - IHSS) and PC (1, 2-bis (10, 12-tricosadiynoyl)-sn-glycero-3-phosphocholine – Avanti Polar Lipid, CAS Registry Number: 76078-28-9).

A precise description of the synthesis procedures of IONP is located in the Supporting Information file (**SI-A**).

2.1.2. Characterization

High Resolution Transmission Electron Microscopy (HR-TEM) was conducted with a JEOL2100F electron microscope (voltage 200 kV) magnNP, maghNP, HA-magnNP and PC-magnNP.

Multipoint N_2–Brunauer Emmett Teller (BET) technique was carried out on magnNP and maghNP using a Coulter (SA 3100) analyzer to measure the surface area of the IONP. BET analyses were not performed on HA- and PC- magnNP because the coated molecules were shown to contain highly narrow microporosity, which adsorbs no N_2 at 77K (Liu et al., 2008, Fu et al., 2015).

Attenuated Total Reflectance-Fourier Transform InfraRed (ATR-FTIR) was performed on magnNP, maghNP, HA-magnNP and PC-magnNP samples in the 650 - 3700 cm^{-1} region using an IS50 Nicolet spectrometer.

Fe(II)/Fe(III) ratio of magnNP and maghNP were determined by the measure of dissolved Fe(II) and Fe(III) concentrations, after acid digestion, using the 1.10 phenanthroline colorimetric method (AFNOR NF T90-017) (Komadel and Stucki, 1988).

The pH-dependent **surface charge (pH_{zpc})** of magnetite was determined by potentiometric acid-base titration using a self-developed titration system with two titrators (794 Basic Titrino - Metrohm).

More information about these characterization techniques can be found in the SI file (**SI-A**).

2.2. Batch reactions

The adsorption experiments investigated the affinity of copper (Cu) for bare magnetite NP (magnNP), HA coated magnetite NP (HA-magnNP), PC coated magnetite NP (PC-magnNP) and maghemite NP (maghNP). Three experiments were conducted to investigate: (i) the Cu adsorption kinetics, (ii) the effect of pH on the Cu adsorption capacity and (iii) the Cu adsorption capacity for the four IONP studied.

2.2.1. Experimental set-up

Copper adsorption kinetic experiments were conducted to determine the equilibration time prior to the Cu adsorption experiments, performed at different pH values and variable Cu

concentrations. The kinetic experiments were performed in triplicate for each IONP in a 0.5 ± 0.05 g L^{-1} solution (400 mL) at pH = 6 with constant Cu = 0.05 mM. The solutions were shaken for 48 h and for each replicate, 10 samples were collected through time. The accurate total Cu and IONP concentrations were controlled for each experiment. Major- and trace-element concentrations were determined by ICP-MS (Agilent 7700x) as described in Demangeat et al. (2018) and using SLRS-5 geostandard (Yéghicheyan et al., 2013). Other aliquots were filtered using ultrafiltration units (2 kDa, cellulose nitrate membranes) and the TE concentrations of the filtrate were determined as the dissolved fractions. Thus, dissolved Cu (< 2 kDa) was considered as non-adsorbed Cu and dissolved Fe was monitored to highlight possible Fe dissolution, which was expected to occur at acidic pH. The results showed that equilibration was achieved within 15 min. All of the following experiments, which lasted several hours, were therefore performed at equilibrium.

To investigate the effect of pH on the Cu adsorption capacity of the IONP, the initial Cu concentration was set at 0.05 mM by diluting a 250 mg L^{-1} Cu stock solution in tubes containing 20 mL of 0.5 g L^{-1} IONP suspension. The pH was adjusted using 0.1 M NaOH or HCl to reach the targeted pH (pH 3, 4, 5, 6 and 7). In the last experiment, Cu was added to 20 mL of 0.5 g L^{-1} IONP suspension in appropriate amounts to obtain concentrations of Cu = 0.5 mM, Cu = 0.1 mM, Cu = 0.05 mM, Cu = 0.01 mM and Cu = 0.005 mM. The pH was adjusted to pH = 6 ± 0.1 using 0.1 M NaOH. Experiments were performed in triplicate for each IONP. After shaking under anaerobic conditions for 18 h, each sample was split into two aliquots to perform the total and dissolved ICP-MS analyses, as previously described.

2.2.2. Adsorption studies

The amount of adsorbed Cu on the four investigated IONP was calculated according to the following equation:

$$\text{Removal efficiency (\%)} = C_0\text{-}C_e/C_0*100 \quad (1)$$

where C_0 (mg L^{-1}) and C_e (mg L^{-1}) are the initial dissolved Cu concentrations and dissolved concentrations of metal ions after adsorption, respectively. The equilibrium adsorption capacity, Q_e (mg g^{-1}) represents the adsorbed Cu per g of IONP and was calculated using the following mass balance equation:

$$Q_e = (C_0 - C_e)V/m \quad (2)$$

where V (L) is the sample volume, and m (g) is the mass of adsorbent.

To parameterize the adsorption behavior of Cu^{2+} onto the IONP, the Langmuir and Freundlich isotherms were employed. Several mathematical models exist to describe the adsorption of molecules and diverse materials onto solid surfaces, and the choice depends on the characteristics of the studied system (Sheng et al., 2010). Langmuir and Freundlich models are commonly used to describe metal ion adsorption equilibrium onto mineral surfaces (Sheng et al., 2010, Panneerselvam et al., 2011, Mamindy-Pajany et al., 2011). The Langmuir model is adapted to describe dynamic equilibrium adsorption processes, assuming that uptake of metal ions occurs on a homogeneous surface by monolayer adsorption and that no interaction exists between the sorbed species. The Langmuir equation is expressed as:

$$C_e/Q_e = 1/(Q°.b) + C_e/Q° \quad (3)$$

where C_e is the concentration of the solute at equilibrium (mg L^{-1}), Q_e is the mass of the contaminant adsorbed per unit weight of the adsorbent (mg g^{-1}), Q° (mg g^{-1}) and b (L mg^{-1}) are constants related to the adsorption capacity and energy of adsorption, respectively.

The Freundlich isotherm describes non-ideal and reversible adsorption. It is commonly used for adsorbents having irregular surface or for single solute systems within a define concentration range (Shaker and Albishri, 2014). The model assumes multilayer adsorption, meaning that different adsorption sites with different adsorption energy exist at the surface of the solid, characterized by non-uniform distribution of adsorption heat and affinities over a heterogeneous surface (Sigg et al, 2011). The Freundlich isotherm is represented as follows:

$$Q_e = K_F \times [C_e]^{1/n} \quad (4)$$

where C_e is the concentration of the solute at equilibrium (mg L^{-1}), Q_e is the mass of the contaminant adsorbed per unit weight of the adsorbent (mg g^{-1}), K_F and n are Freundlich constants which relate to the adsorption capacity and to the degree of dependence of adsorption at equilibrium concentration, respectively. When it is expressed in the logarithmic form, Equation (4) gives:

$$\log Q_e = \log K_F + (1/n) \log C_e \quad (5)$$

The adsorption data were plotted according to Equation (3) (Langmuir model) and (5) (Freundlich model) using the Cu concentrations obtained in triplicates in the last experiment. The adsorbent concentrations in the solutions were equal to 0.5 g L^{-1} and the pH was adjusted to pH = 6.

2.3. Cu speciation

Copper speciation in the presence of IONP was investigated using Visual Minteq 3.1. In particular, the concentration of the different Cu species was calculated relative to the pH in our experimental conditions (21 °C, 0.005 M NaCl). The model considered the presence of IONP (0.5 g L^{-1}) including the properties of IONP determined from the BET analyses and potentiometric titration (i.e. number of adsorption sites, pKa_1 and pKa_2). From the potentiometric titration experiment conducted at NaCl = 0.005 M, we calculated pKa_1=4.6 and pKa_2=7.8 for magnNP. For maghNP, pKa_1=5.4 and pKa_2=9.3 were estimated from literature considering maghemite nanoparticles with similar properties as those used in this study (Jarbling et al., 2005). The surface site density of IONP, Ns = 1.59 ± 0.05 sites per nm^2 was calculated from potentiometric titration of magnNP based on the Granplot method (Jolstera et al., 2012, Cheng et al., 2018). The obtained value is close to those found in previous works using the same method (Jolstera et al., 2012, Cheng et al., 2018, Lucas et al., 2007). The stability constant was deduced from the best fit obtained between experimental data and modelled data at logK= 0.6.

The sorption constant was fitted using the experimental datasets of the adsorption isotherm experiments. The best fit was validated by the calculation of the RMSE. Calculations were performed at pH values ranging from 3 to 8 to obtain the concentrations of the significant Cu species (Cu^{2+}, $CuOH^{+}$, $Cu(OH)_2(aq)$, $Cu(OH)^{3-}$, $Cu_3(OH)_4^{2+}$, $Cu(OH)_2(s)$) as well as the saturation index of the possible Cu solids ($Cu(OH)_2(s)$, Tenorite). The adsorption of Cu onto HA-magnNP and PC-magnNP was not modeled because Visual Minteq3.1 considers HA and PC as additional ligands instead of surface materials.

3. Results and discussion

3.1. Impacts of oxidation and surface coating on magnNP

3.1.1. IONP physicochemical properties

Magnetite and maghemite. As determined from the HR-TEM analyses (**SI-B**), maghNP were spherical and had a mean diameter close to 7 ± 2 nm. Although the transformation of magnNP into maghNP did not show any change in size, the BET measurements highlighted an increase in the surface area from 115 ± 4 m^2 g^{-1} before oxidation (magnNP) to 130 ± 4 m^2 g^{-1} after oxidation (maghNP). It has further been demonstrated that maghemite has a disordered crystal structure in which vacancies could favor cation scavenging (Frison et al., 2013, Gorski et al., 2010). On another hand, the Fe(II)/Fe(III) ratio of magnNP in the adsorption experiment decreased from 0.38 ± 0.02 at the beginning of the experiment to 0.34 ± 0.02 after the interaction, corresponding to non-stoichiometric magnetites (Schwaminger et al., 2017, Lohdia et al., 2010). The Fe(II)/Fe(III) ratio is worth considering as it has an influence on the interactions with the surrounding dissolved species, as Fe(II) likely facilitates the transfer of electrons (Auffan et al., 2008). In a previous study, we showed that after nine days Fe(II)/Fe(III) rapidly decreased to Fe(II)/Fe(III) = 0.1 in aerobic conditions due to oxidation of magnetite into maghemite (Demangeat et al., 2018). In the present study, the Fe(II)/Fe(III) ratio of maghNP was measured at 0.05 ± 0.02. Besides, the pHzpc of magnNP obtained from potentiometric titration experiment gave a pHzpc=6.2 whereas the pHzpc of maghNP was determined at 7.35.

HA- and PC- coated magnetite. Neither HA nor PC coatings induced any significant size change, indicating that the modifications occurred at the surface of magnNP (Fu et al., 2015, Koesnarpadi et al., 2015). According to the obtained infrared spectra (**SI-C**), PC- and HA-magnNP have bands of pure PC and HA, respectively, as well as bare magnNP, which support the successful coating of PC and HA, respectively, onto the oxide surface (Niu et al., 2011). In the spectra of Fe_3O_4-PC, as observed in pure PC sample, the absorption bands at 2849 cm^{-1} and 2940 cm^{-1} were assigned to symmetric and asymmetric methylene (CH_2) and methyl (CH_3) vibrations, respectively (Debnath et al., 2010). The bands at 1272 cm^{-1}, 1088 cm^{-1}, 970 cm^{-1} and 820 cm^{-1} were attributed to the presence of PO_4^{3-} group onto magnetite surface (Debnath et al., 2010), and those at 1470 cm^{-1} and 1412 cm^{-1} were ascribed to CH_2 scissoring. The anchoring of PO_4^{3-} supports the successful coating of PC on magnNP surface, most likely via chemisorption, which involves the covalent binding between the phosphate groups and the hydroxyl groups of magnNP (Le et al., 2014). In the spectra of HA-magnNP, the band at ~1614 cm^{-1} was attributed to the sorption of carboxylates onto the magnetite surface. This absorption band likely resulted from the shift, after its binding to the FeO, of the 1709 cm^{-1} vibration band (C=O stretch of free

carboxylic acid) observed in pure HA spectra. The band at 1410 cm^{-1} could be related to COO^- symmetric stretch (Demirel et al., 2006). HA is likely fractionated during its adsorption to the magnNP and it has been demonstrated that low molecular weight, –O and –N rich functional groups would preferentially adsorbed onto the IONP surface. These smaller size-fractions would display enhanced probability for ligand-exchange reactions (Illès and Tombacz, 2004). Indeed, the binding of carboxylate with the surface hydroxyl site of iron oxide has been reported to involve ligand exchange mechanism (Liu et al., 2008, Maity and Agrawal, 2007). The surface chemical modifications induced by HA and PC coatings to magnNP are relevant regards to the numerous interactions occurring between IONP and the solution constituents, including metal ions. Indeed, if the same sites for binding HA and metals are used, the binding of HA directly on mineral surface may hamper metal sorption due to the site blockage and competition. If not, the binding of HA at the IONP surface can become favorable to the uptake of metals because of the complexation between HA and metals.

3.1.2. Chemical stability of IONP

The increased Fe concentrations (dissolved Fe measurements) highlighted the preferential dissolution of magnNP at acidic pH **(Table 1)**. After 18 hours, dissolved Fe accounted for 1.5% of the total Fe content in magnNP at pH = 3 and it decreased to 0.4% when the pH increased to pH = 4. These values fall in the range of previously reported dissolved Fe concentrations in close experimental conditions (Missana et al., 2009). However, the time of the experiment being much shorter in our study compared with that of Missana et al. (2009), it appears that the dissolution rate was much higher for the 7-nm-sized magnNP than for the 50-200 nm magnetite nanocrystals of Missana's work. Previous studies have indeed highlighted that increased dissolution rate preferentially occurred to smaller-sized particles (Mudunkotuwa and Grassian, 2011, Liu et al., 2009). MaghNP displayed a lower amount of released Fe than magnNP, from 0.43% at pH = 3 to 0.09% at pH = 4. The decrease in released Fe between magnNP and maghNP stemmed from the different compositions of both Fe oxides. While maghemite only contains Fe(III) in its structure, magnetite (Fe_3O_4) also contains Fe(II), which is a much more soluble species than Fe(III) (Jolstera et al., 2012, Maity and Agrawal, 2007). Therefore, magnetite is prone to higher Fe leaching than maghemite, which has previously been observed (Jolstera et al., 2012). The transformation of magnetite to maghemite stems from the solubilization of Fe(II). In our study,

the dissolved Fe concentrations were negligible for PC-magnNP and HA-magnNP at acidic pH, suggesting that dissolution was almost ineffective at low pH values, and thus, that the transformation of magnetite into maghemite was reduced in the presence of these organic coatings. From these observations, we inferred that PC and HA yield comparable protecting effects against IONP dissolution, probably related to the presence of an efficient barrier at the surface of magnNP (Scherer and Neto, 2005, Lu et al., 2007). Nevertheless, another possibility is that HA and PC surface coatings can provide binding sites to dissolved Fe (Peng et al., 2019, Catrouillet et al., 2014). Re-adsorption of aqueous Fe would limit the measured total dissolved Fe content, as observed from the ICP-MS measurements performed in the present study. Although different modes of interaction have been proposed to explain the adsorption of HA and PC onto magnNP, it is likely that several mechanisms are involved, and their relative contribution may vary depending on the intrinsic properties of the organic molecules, those of magnNP and those of the solution chemistry as well. In our study, the coating of magnNP by HA was performed at basic condition in order to increase HA resistance to leaching. Although low pH promotes HA attraction to positively charged iron oxide surface, the formation of specific surface complexes onto mineral surfaces can effectively be achieved even if the oxide surfaces and the organic molecules are both negatively charged (Aiken et al., 2011, Yu et al., 2018). At high pH, HA exists in a rather linear or stretched structure which favors multiple sites binding with magnetite, and by the same, reduce the Fe and HA leaching from HA-coated magnetite (Liu et al., 2008, Grillo et al., 2015). According to Liu et al (2008), Fe and HA leaching would be negligible and undergo only slight modification after 6 hours (0.03% and 1.3% respectively), 12 hours (0.07% and 3.5% respectively) and 12 days (0.21% and 0.33% respectively). Results of this study were based on the concentration of Fe and DOC in the supernatant obtained from the resuspension of HA-coated magnetite NP in deionized water (constant pH = 6) over different periods of time. It is corroborated to other studies, which showed that the leaching of HA from iron oxide is generally negligible in tap waters and deionized waters (Gu et al., 1994).

3.2. How do magnNP modifications constrain Cu adsorption?

3.2.1. Effects of pH on Cu adsorption

MagnNP. For bare magnNP and Cu = 0.05 mM, the percentage of Cu adsorbed (Cu% adsorbed) increased with the increasing pH **(Figure 1)**. In compliance with the measured pH_{zpc} =

6.2, the Cu% adsorbed at pH > pH_{zpc} (at pH 6 and 7) was high (almost 100% Cu adsorbed) as compared to the weak Cu% adsorbed (<10% Cu adsorbed) at low pH (pH 3 and 4). At pH > pH_{zpc}, the IONP surfaces became negatively charged resulting from deprotonation reactions. The decreasing protons concentration at magnetite surface favors cation attraction and allows Cu^{2+} to complex onto the FeO^- surface sites (Madden et al., 2006, Huang and Chen, 2009). According to ATR-FTIR analyses performed on magnNP after Cu addition (Cu = 0.5 mM) (**SI-D**), the adsorption of Cu onto magnNP was discernable by the vibration at 1350 cm^{-1}. This absorption band was observed in the IR spectrum obtained for Cu in the solution, and in the IR spectrum of magnNP/Cu at pH 5, 6, 7 and 8, whereas no absorption band was recorded at 1350 cm^{-1} in the IR spectrum of bare magnNP (before Cu addition). On the contrary, the IR spectrum of magnNP/Cu at pH 3.5 resembled that of magnNP before NP/Cu interaction, with no absorption band at 1350 cm^{-1} suggesting that no Cu was adsorbed on magnNP surface at pH 3.5. The broad band at 3150 - 3400 cm^{-1} and the band at circa 1630 cm^{-1} are characteristic of, respectively, the stretching and bending vibration of hydroxyl groups at the surface of magnNP (Maity and Agrawal, 2007, Ahmad et al., 2012) and their intensity is clearly decreased with increasing pH as deprotonation occurs and Cu^{2+} ions are adsorbed onto the surface of the adsorbent. ATR-FTIR results are consistent with previous ICP-MS data, highlighting that Cu adsorption is favored at pH ≥ 5 and thus that protonation/deprotonation reaction is a major mechanism controlling Cu sorption onto magnNP.

MaghNP. Cu adsorption onto maghNP followed the same trend as on magnNP, and Cu% adsorbed increased with increasing pH. Therefore, magnetite and maghemite likely had similar surface properties. In particular, as magnNP is not perfectly stoichiometric, it is suggested that its surface is partially oxidized. Hence, fully oxidized maghemite and partially surface-oxidized-magnetite displayed similar adsorption capacity for Cu. Furthermore, since no improvements in Cu sorption onto maghemite were observed, the surface area increase observed after oxidation did not enhance the adsorption of Cu, which was expected to increase. To address this issue, Jarbling et al. (2005) proposed that the increased surface area was related to the microporous surface structure of maghemite, which includes non-active surface sites. On another hand, surface area determined by BET measurements was conducted at a favorable pH to form stable maghemite suspension, whereas magnetite likely aggregated at the same pH. Thus, the surface area of magnNP might have been lowered due to its aggregation during the measurements.

PC-magnNP. The results for PC-magnNP showed that Cu adsorption started from pH = 4 (4% Cu adsorbed) and reached its maximum at pH = 6 (100% Cu adsorbed), hence following the same trend as for bare magnNP. In fact, PC anchoring did not modify the pH_{zpc} of magnNP in a great extent as PC is electrically neutral at pH = 7. The pH-dependency of Cu adsorption onto PC-magnNP may yet remain on the zwitterionic head group in PC (containing a positively charged trimethylethanolammonium group and a negatively charged glycerophosphate group), which likely created a dipole, impacted the surface hydration of the NP and thus the interaction with Cu (Shinoda, 2016). In this frame, Cu could coordinate with the electronegative oxygen in the carbonyl group deeper in the bilayer as was reported for Zn^{2+} (Alsop et al., 2016). Furthermore, cation binding is expected to occur more or less close to the phosphate group (or to the glycerol group) possibly depending on the size of the ion. Divalent Ca^{2+} was found to coordinate and bind electrostatically with oxygen molecules on four adjacent lipid molecules, whereas Mg^{2+} bound closer to the phosphate group and coordinated with water oxygens (Melcrová et al., 2016). Thus, the PC coating does not necessarily represent a barrier to metal cations and therefore Cu could bind to some of the PC functional groups. Nevertheless, it is still difficult to specify the interaction between Cu and PC-magnNP as it is not known whether PC encapsulated the whole surface of magnNP or if it formed patchy coatings around the magnNP (leaving some of the magnNP surfaces lipid-free).

HA-magnNP. Copper adsorption onto magnNP coated with HA rapidly increased with the increasing pH. The rapid removal capacity of Cu^{2+} by HA-magnNP shows that HA provided readily accessible sorption sites to Cu^{2+}. It is believed that HA improve metal adsorption in HA-coated NP by providing numerous phenolic and carboxylic groups to HA-coated NP (Illès and Tombacz, 2004, Gomes de Melo et al., 2016). Besides, the surface chemical modifications induced by HA coating likely lowered the pH_{zpc} of bare magnNP because of the acidic oxygen-containing functional groups content (Liu et al., 2008, Gomes de Melo et al., 2016, Peng et al., 2012, Chekli et al., 2013). HA pH_{zpc} is close to pH = 2.3 (Liu et al., 2008). Hence, Cu^{2+} adsorption onto HA-magnNP was favored when the pH increased. Decreased pH_{zpc} resulting from HA coating was shown to favor the adsorption of several metals (such as Cu(II), Cd(II), Hg(II), Pb(II), Zn(II)) since HA imparted negative surface charge to IONP which increased the affinity of mineral surfaces for cations over a wide pH range (Liu et al., 2008, Illès and Tombacz, 2004, Lin et al., 2011). On the other hand, HA likely formed a network around coated magnNP

which could influence the aggregation of the IONP, especially with increased time exposure, and favors metal trapping and adsorption (Zhang et al., 2009, Liu et al., 2008). Hence, the adsorption capacity of HA-coated magnetite is generally higher than that of magnNP and HA alone. The effects of pH on HA own conformation also do play an important role in driving HA / metals interactions. In fact, HA exists in a rather linear or stretched structure at high pH, which favors multiple sites binding with inorganic species including Cu cations (Liu et al., 2008; Grillo et al., 2015). Furthermore, results show that adsorbed Cu% to HA-magnNP was high even at acidic pH (**Figure 1**). Hence, HA likely promoted the adsorption of Cu^{2+} to HA-magnNP through the formation of strong complexes, with a covalent character, and resistant against proton exchange (Kostic et al., 2011; Senesi et al., 1986). In fact, it was shown that most Cu species bind to HA by forming inner-sphere complexes with the acidic functional groups in HA, although binding through hydrated outer-sphere surface complexes is also expected under favorable conditions (Li et al., 2015; Komy et al., 2014; Otero-Farina et al., 2015).

3.2.2. Adsorption isotherms

The adsorption data were fitted with the Langmuir and Freundlich adsorption equations to determine the adsorption parameters and the consistency with the models. The Freundlich adsorption model provided the best fit regarding the experimental results (**SI-E**) with higher R^2 obtained for the four IONP investigated. The calculated linear regression coefficients (R^2) calculated from Freundlich linearized plots were higher than 0.95 suggesting a strong linear relationship between log Q_e and log C_e (**SI-F**). The obtained K_F and n values are comparable to the Freundlich parameters reported in previous studies (Kakavandi et al., 2015; Karami, 2013). The K_F data highlight the highest affinity of Cu to HA-magnNP (in the following order of affinity: HA-magnNP >> maghNP > PC-magnNP = magnNP). The values decreased in the range usually reported for the adsorption of trace metals onto nanomaterials in aqueous solution (Vatta et al., 2006). For the n parameter, the values lie between 1 and 10, indicating a favorable and specific adsorption (chemisorption) of Cu to the IONP over the entire range of Cu concentration investigated. In particular, the adsorption isotherm of HA-magnNP was implemented based on the obtained high n value (**SI-G**), highlighting a high heterogeneity in the process of Cu sorption to HA-magnNP (Xu et al. 2012; Li et al., 2015). Metals, including Fe and Cu, can be held to very strong binding sites onto humic substances. It was already reported (Tipping, 2002) that the

sorption between HA and metals formed complexes with either the carboxylic and phenolic groups of HA or through specific binding between metals and the N and S groups of HA. Therefore, the heterogeneous adsorption between HA-magnNP and Cu can be explained by both the diversity of the binding sites provided by HA and the formation of multidendate complexes between Cu and some HA functional groups.

3.2.3. Cu speciation

Copper speciation was studied relative to the pH, at three Cu concentrations (Cu = 0.05 mM, Cu = 0.1 mM and Cu = 0.5 mM) and taking into account the leaching of Fe (**SI-H**). At the lowest Cu concentration (Cu = 0.05 mM), Cu speciation displayed the same pattern with magnNP and maghNP. Dissolved Cu^{2+} was the predominant species up to pH = 5. Beyond this pH, most of the Cu was bound to the surface of the IONP and most of the dissolved Cu species occurred in minor amounts (< 1.10^{-5} mM). When the initial Cu concentration increased up to Cu = 0.5 mM, Cu^{2+} was the dominant species until pH = 6.5. Copper adsorption occurred from pH 4 to 6.5. Cu precipitation was expected as the pH reached 6.5, as observed in previous studies (Hidmi and Edwards, 1999; Boukhalfa et al., 2007, Balintova and Petrilakova, 2011).

Several conclusions can be drawn from the speciation calculation and the present results:

- the pH edges obtained for magnetite and maghemite at Cu = 0.05 mM turned out to be consistent with our results showing an increasing adsorbed Cu% with the increasing pH (pH > 4);
- the decreasing adsorbed Cu%, observed with the increasing Cu concentrations, was both related to the precipitation of Cu and, mostly, to the surface site saturation of magnNP;
- no Cu precipitation was expected for Cu = 0.05 mM, whereas the increasing Cu concentration up to Cu = 0.5 mM induced saturation and precipitation at pH values above 6.5;
- modeled data displayed a good consistency with our experimental results and therefore the use of the diffuse layer surface complexation model, along with the characteristics of the IONP, could be used to predict Cu dynamics in the presence of IONP.

3.3. Environmental implications

3.3.1. Impacts of IONP dissolution on the IONP stability and solution chemistry

IONP dissolution is relevant regards to several environmental issues (Goswani et al., 2017). From the nanoparticle perspective, IONP dissolution is expected to favor the formation of smaller-sized IONP with new intrinsic properties as compared with pristine particles (Mudunkotuwa and Grassian, 2011). Increase in the surface free energy (Guzman et al., 2006), resulting from IONP size decrease, could favor the aggregation of IONP. Nevertheless, the last hypothesis was not verified in our study since magnNP dissolution occurred at pH=3 and pH=4, which refers to pH where magnNP are less aggregated (**Figure 1**). On another hand, aggregation of IONP could limit their dissolution by forming larger bulk particles (thereby decreasing the surface contact in between the IONP) (Mudunkotuwa and Grassian, 2011). Dissolution of IONP resulting from pH decrease (proton-promoted dissolution) also induced Fe release in the solution. The presence of dissolved Fe could modify the solution chemistry and influence the stoichiometry, reactivity and recrystallization of magnNP in aqueous environments (Gorski et al., 2010). Doing so, the release of Fe(II) induced by IONP dissolution plays a key role in a wide range of biogeochemical processes (Byrne et al., 2015, Peng et al., 2018, Peng et al., 2019). Fe(II) interactions with IONP are also of great concern in several environmental applications such as remediation, by influencing the mobility and the redox state of heavy metals (Gorski et al., 2012). Besides, IONP dissolution can also directly control TE release in the environment and lead to some more interactions with aqueous Fe or other dissolved species (complexation, precipitation, etc.) upon certain environmental conditions (Bhatt and Tripathi, 2011). And these interactions may become more complex in the presence of other ligands such as HA (Aiken et al., 2011, Pédrot et al., 2011) since HA can prevent mineral precipitation, even at high cation concentration and high pH, by increasing cations adsorption (which decreased the saturation index of metal).

3.3.3. Is there any link in between IONP aggregation and Cu adsorption?

In a previous study, we inferred that, in addition to pH, the surface area and surface chemistry (HA and PC coatings) turned out to be key drivers in controlling the aggregation of IONP (Demangeat et al., 2018), resulting mainly from electrostatic and combined electrosteric interactions. In the present study, the observations of Cu adsorption onto IONP showed that adsorption was likely dependent upon the available active sites for Cu. Nevertheless, the

distribution, density and surface binding geometries may vary with the morphology of the aggregates (Gilbert et al., 2009). Therefore, the aggregation of IONP was expected to influence Cu adsorption. By correlating aggregates' sizes, Cu adsorption and pH, no clear relationship can be established between IONP aggregation and Cu adsorption capacities (**Figure 1**). For magnNP, in particular, although adsorption experiments showed that increasing pH lead to increasing Cu adsorption, the aggregation study highlighted that larger magnNP aggregates were formed at pH > 5. In a previous study (Demangeat et al., 2018), the same size-distribution were observed at pH 3, 4 and 5 (with about 80% of magnNP being particles with diameter ≤ 100 nm) whereas, in the present study, the proportion of adsorbed Cu increased when pH increased from pH 4 to pH 5. Thus, the proportion of Cu is modified regardless of magnNP colloidal state. Furthermore, the proportion of these small size particles (with diameter ≤ 100 nm) diminished to 65% at pH 6 and 7.5, the optimum pH for Cu adsorption in the present work. Hence, instead of diminishing the available reactive surface, aggregation did not prevent Cu from being adsorbed onto those bigger particles. We therefore hypothesized that the aggregation of IONP would rest on weak attraction forces and result in the formation of loosely packed aggregates, without any loss of reactive surface area.

Although no clear link is concluded regarding the impact of IONP colloidal behavior on Cu adsorption capacity, IONP colloidal stability may still have an impact on Cu dynamics. It was shown that less aggregation between IONP yielded lower rates of sedimentation and increased the mobility of adsorbed cations (Ju-Nam and Lead, 2008). Consequently, rather than being involved directly within the adsorption step, IONP colloidal stability could play a key role in Cu transport, mobility, bioavailability and toxicity once the metal is bound to the IONP (Baumann et al., 2014, Bottero et al., 2011).

4. Conclusion

IONP can undergo many changes in natural waters and soils. In this study, oxidation of magnetite and HA and PC natural organic coatings induced surface changes that affected both the behavior of the IONP in aqueous solution and the interactions occurring at oxide/water interface. In term of Cu adsorption capacity, the structural and chemical diversity of HA decreased the pH_{zpc} of HA-magnNP and provided a large amount of hydrophobic and heteroaliphatic functional groups, which also favored the formation of strong surface complexes onto HA-magnNP over a

wide pH-range. Contrary to HA-magnNP, PC-magnNP and maghNP displayed similar behavior than pristine magnNP showing that neither PC coating nor magnNP oxidation affected Cu adsorption capacity. On another hand, both HA and PC surface coatings prevented Fe release from the IONP at low pH. Oxidation of mixed-oxidation state magnNP to maghNP also considerably reduced its dissolution rate, suggesting that Fe^{2+} in magnNP is more soluble than Fe^{3+} in maghNP. Last, if aggregation did not affect the adsorption of Cu, it could be secondarily involved in driving the metal fate by impacting its speciation and thus its mobility and solubility. Deciphering the interactions between IONP, cations and organic molecules as well as investigating the behavior and fate of IONP in the environment (aggregation, transport, toxicity) could have strong implications towards diverse scientific issues including water quality, agronomics, and environmental remediation.

Acknowledgments

We are thankful to A. Beauvois for his kind help to perform potentiometric titrations and Dr R. Marsac for the thorough advice he gave to build the models. We are also grateful to Dr. K. Hanna for providing access to the analytical facilities in his laboratory. This study was funded by the CNRS-INSU/INEE EC2CO and the Interdisciplinary Mission programs through the 'NanoOrgaTraces' and 'ALIEN' projects, awarded to Dr M. Pédrot and the University of Rennes, respectively, through the "Défis Scientifiques Emergents" program awarded to Dr A. Dia. Dr S. Mullin is acknowledged for post-editing the English style (http://www.proz.com/profile/677614).

References

Adrees, M., Ali, S., Rizwan, M., Ibrahim, M., Abbas, F., Farid, S., Zia-ur-Rehman, M., Irshad, M.K., Bharwana, S.A., 2015. The effect of excess copper on growth and physiology of important food crops: a review. Environ. Sci. Pollut. Res. 22, 8148-8162. http://dx.doi.org/10.1007/s11356-015-4496-5

Afkhami, A., Saber-Tehrani, M., Bagheri, H., 2010. Modified maghemite nanoparticles as an efficient adsorbent for removing some cationic dyes from aqueous solution. Desalinisation 263, 240-248. http://dx.doi.org/10.1016/j.desal.2010.06.065

Ahmad, R., Kumar, R., Haseeb, S., 2012. Adsorption of Cu^{2+} from aqueous solution onto iron oxide coated eggshell powder: Evaluation of equilibrium, isotherms, kinetics and regeneration capacity. Arabian J. Chem. 5, 353-359. https://doi.org/10.1016/j.arabjc.2010.09.003

Ahmed, M.A., Ali, S.M., El-Dek, S.I., Galal, A., 2013. Magnetite-hematite nanoparticles prepared by green methods for heavy metal removal from water. Mater. Sci. Eng., B 178, 744-751. http://dx.doi.org/10.1016/j.mseb.2013.03.011

Aiken, G.R., Hsu-Kim, H., Ryan, J.N., 2011. Influence of Dissolved Organic Matter on the environmental Fate of Metals Nanoparticles, and Colloids. Environ. Sci. Technol. 45, 3196-3201. http://dx.doi.org/ 10.1021/es103992s

Alsop R.J., Schober, R.M., Rheinstädter, M.C., 2016. Swelling of phospholipid membranes by divalent metal ions depends on the location of the ions in the bilayers, Soft Matter 12, 6737-6748. http://dx.doi.org/10.1039/c6sm00695g

Made M., Liu, J.F., Tan, Z.O., Bekana, D., 2017. Transformation and bioavailability of metal oxide nanoparticles in aquatic and terrestrial environments, A review. Environ. Pollut. 230, 250-267. http://dx.doi.org/10.1016/j.envpol.2017.06.064

Auffan, M., Achouak, W., Rose, J., Roncato, M.A., Chanéac, C., Waite, D.T., Mason, A., Woisik, J.C., Wiesner, M.R., Bottero, J.Y., 2008. Relation between the redox state of iron-based nanoparticles and their cytotoxicity toward Escherichia coli. Environ. Sci. Technol. 42, 6730-6735. http://dx.doi.org/10.1021/es800086f

Balintova, M., Petrilakova, A., 2011. Study of pH Influence on Selective Precipitation of Heavy Metals from Acid Mine Drainage. Chemical Engineering Transactions 25, 345-350. http://dx.doi.org/10.3303/CET1125058

Baumann, J., Köser, J., Arndt, D., Filser, J., 2014. The coating makes the difference: Accute effects of iron oxide nanoparticles on Daphnia magna. Sci. Total Environ. 484, 176-184. http://dx.doi.org/10.1016/j.scitotenv.2014.03.023

Bhatt, I., Tripathi, B.N., 2011. Interaction of engineered nanoparticles with various components of the environment and possible strategies for their risk assessment. Chemosphere 82, 308-317. http://dx.doi.org/10.1016/j.chemosphere.2010.10.011

Bottero, J.Y., Auffan, M., Rose, J., Mouneyrac, C., Botta, C., Labille, J., Masion, A., Thill, A., Chaneac, C., 2011. Manufactured metal and metal-oxide nanoparticles: properties and perturbing mechanisms of their biological activity in ecosystems. C.R. Geosci. 343, 168-176. http://dx.doi.org/10.1016/j.crte.2011.01.001

C. Boukhalfa, A. Mennour, L. Reinert, M. Dray, L. Duclaux, 2007. Removal of copper from aqueous solution by coprecipitation with Hydrated Iron Oxide. Asian J. Chem. 19 (6), 4267-4276.

Jr Brown, G.E., Henrich, V.E., Casey, W.H., Clark, D.L., Eggleston C., Felmy A., Goodman, D.W., Grätzel, M., Maciel, G., McCarthy, M.I., Nealson, K.H., Sverjensky, D.A., Toney M.F.,

Zachara J.M., 1999. Metal Oxide Surfaces and Their Interactions with Aqueous Solutions and Microbial Organisms. Chem. Rev. 99(1), 77-174. https://doi.org/10.1021/cr980011z

Byrne, J.M., Klueglein, N., Pearce, C., Rosso, K.M., Appel, E., Kappler, A., 2015. Redox cycling of Fe(II) and Fe(III) in magnetite by Fe metabolizing bacteria. Science 347, 1473-1476. http://dx.doi.org/10.1126/science.aaa4834.

Catrouillet, C., Davranche, M., Dia, A., Bouhnik-Le Coz, M., Marsac, R., Pourrret, O., Gruau, G., 2014. Geochemical modeling of Fe(II) binding to humic and fulvic acids. Chem. Geol. 372, 109-118. http://dx.doi.org/10.1016/j.chemgeo.2014.02.019

Chekli, L., Phuntsho, S., Roy, M., Shon, H.K., 2013. Characterization of Fe-oxide nanoparticles coated with humic acid and Swannee River natural organic matter. Sci. Total Environ. 461-462, 19-27. http://dx.doi.org/ 10.1016/j.scitotenv.2013.04.083

Cheng, W., Marsac, R., Hanna, K., 2018. Influence of magnetite stoichiometry on the binding of emerging organic contaminants. Environ. Sci. Technol. 52(2), 467-473. http://dx.doi.org/10.1021/acs.est.7b04849

Christl, I., Kretzschmar, R., 2001. Interaction of copper and fulvic acid at the hematite – water interface. Geochim. Cosmochim. Acta (65) 20, 3435-3442. https://doi.org/10.1016/S0016-7037(01)00695-0

Dabrowski, A., Hubicki, Z., Podkoscielny, P., Robens, E., 2004. Selective removal of the heavy metal ions from waters and industrial wastewaters by ion-exchange method. Chemosphere 56, 91-106. http://dx.doi.org/10.1016/j.chemosphere.2004.03.006

Davranche, M., Dia, A., Fakih, M., Nowack, B., Gruau, G., Ona-Nguema, G., Petitjean, P., Martin, S., Hochreutener, R., 2013. Organic matter control on the reactivity of Fe(III)-oxyhydroxides and associated As wetland soils: a kinetic modeling study. Chem. Geol. 335, 24-35. http://dx.doi.org/10.1016/j.chemgeo.2012.10.040

Debnath, S., Hausner, D.B., Strongin, D.R., Kubicki, J., 2010. Reducive dissolution of ferrihydrite by ascorbic acid and the inhibiting effect of phospholipids. J. Colloid Interface Sci. 341, 215-223. http://dx.doi.org/10.1016/j.jcis.2009.09.035

Demangeat, E., Pédrot, M., Dia, A., Bouhnik-le-Coz, M., Grasset, F., Hanna, K., Kamagaté, K., Cabello-Hurtado, F., 2018. Colloidal and Chemical stabilities of iron oxide nanoparticles in aqueous solutions: the interplay of structural, chemical and environmental drivers. Environ. Sci. Nano, 5, 992-1001. http://dx.doi.org/10.1039/c7en01159h

Demirel, C.U., Bekbolet, M., Swietlik, J., 2006. Natural organic matter: definitions and characterization. Publishers, Nova Science Chap 5.1., 25pp. Inc. ISBN 1-60021-322-7

627 Frison, R., Cernuto, G., Cervellino, A., Zaaharko, O., Colonna, G.M., Guagliardi, A.,
628 Masciocchi, N., 2013. Magnetite-Maghemite Nanoparticles in the 5-15 nm range: correlating the
629 core-shell composition and surface structure to the magnetic properties. A total scattering study.
630 Chem. Mater. 25, 4820-4828. http://dx.doi.org/10.1021/cm403360f

631 Fu, Q., Zhou, X., Xu, L., Hu, B., 2015. Fulvic acid decorated Fe_3O_4 magnetic nanocomposites for
632 the highly efficient sequestration of Ni(II) from an aqueous solution. J. Mol. Liq. 208, 92-98.
633 http://dx.doi.org/10.1016/j.molliq.2015.04.017

634 Ghosh, S., Jiang, W., McClements, J.D., Xing, B., 2011. Colloidal Stability of Magnetic Iron
635 Oxide nanoparticles: Influence of Natural Organic Matter and Synthetic Polyelectrolytes.
636 Langmuir 27, 8036-8043. http://dx.doi.org/10.1021/la200772e

637 Gilbert, B., Ono, R.K., Ching, K.A., Kim, C.S., 2009. The effects of nanoparticles aggregation
638 processes on aggregates structure and metal uptake. J. Colloid Interface Sci. 339, 285-295.
639 http://dx.doi.org/10.1016/j.jcis.2009.07.058

640 Giri, J., Thakurta, S.G., Bellare, J., Nigam, A.K., Bahadur, D., 2005. Preparation and
641 characterization of phospholipid stabilized uniform sized magnetite nanoparticles. J. Magn.
642 Magn. Mater. 293, 62-68. http://dx.doi.org/10.1016/j.jmmm.2005.01.044

643 Gomes de Melo, B.A., Motta, F.L., Santana, M.H.A, 2016. Humic acids: Structural properties
644 and multiple functionalities for novel technological developments. Mater. Sci. Eng., C 62, 967-
645 97. http://dx.doi.org/10.1016/j.msec.2015.12.001

646 Gorski, C.A., Nurmi, J.T., Tartneyk, P.G., Hofstetter, T.B., Sherer, M.M., 2010. Redox behaviour
647 of magnetite: implications for contaminant reduction. Environ. Sci. Technol. 44, 55-60.
648 http://dx.doi.org/10.1021/es9016848

649 Gorski, C.A., Handler, R.M., Beard, B.L. Pasakarnis, T., Johnson, C.M., Sherer, M.M., 2012. Fe
650 atom exchange between aqueous Fe^{2+} and magnetite. Environ. Sci. Technol. 46, 12399-12407.
651 http://dx.doi.org/10.1021/es204649a

652 Goswani, L., Kim, K.H., Deep, A., Das, P., Bhattacharya, S.S., Kumar, S., Adelodun, A.A., 2017.
653 Engineered nanoparticles: Nature, behavior, and effect on the environment. J. Environ. Manage.
654 196, 297-315. http://dx.doi.org/10.1016/j.jenvman.2017.01.011

655 Grillo, R., Rosa, A.H, Fraceto, L.F., 2015. Engineered nanoparticles and organic matter: A
656 review of the state-of-the-art. Chemosphere 119, 608-619.
657 http://dx.doi.org/10.1016/j.chemosphere.2014.07.049

658 Gu, B., Schmitt, J., Chen, Z., Liang, L., McCarthy, J.F., 1994. Adsorption and desorption of
659 natural organic matter on iron oxide: mechanisms and models. Environ. Sci. Technol. 28, 38-46.
660 http://dx.doi.org/10.1021/es00050a007

661 Gupta, A.K., Gupta, M., 2005. Synthesis and surface engineering of iron oxide nanoparticles for
662 biomedical applications. Biomaterials 26, 3995-4021.
663 http://dx.doi.org/10.1016/j.biomaterials.2004.10.012

664 Guzman, KAD., Finnegan, M.P., Banfield, J.F., 2006. Influence of surface potential on
665 aggregation and transport of titania nanoparticles. Environ. Sci. Technol. 40, 7688-7693.
666 http://dx.doi.org/10.1021/es060847g

667 Hadju, A., Illès, E., Tombacz, E., Borbath, I., 2009. Surface charging, polyanionic coating and
668 colloid stability of magnetite nanoparticles. Colloids Surf., A 347, 104-108.
669 http://dx.doi.org/10.1016/j.colsurfa.2008.12.039

670 Hidmi, L., Edwards, M., 1999. Role of temperature and pH in $Cu(OH)_2$ solubility. Environ. Sci.
671 Technol. 33 (15), 2607–2610. http://dx.doi.org/10.1021/es981121q

672 Hu, J., Chen, G., Lo, I.M.C., 2005. Removal and recovery of Cr(VI) from wastewater by
673 maghemite nanoparticles. Water Res. 39, 4528-4536.
674 http://dx.doi.org/10.1016/j.watres.2005.05.051

675 Hu, J., Chen, G., Lo, I.M.C., 2006. Selective removal of heavy metals from industrial wastewater
676 using maghemite nanoparticles: performance and mechanisms. J. Environ. Eng. 132, 709-715.
677 http://dx.doi.org/10.1061/(ASCE)0733-9372(2006)132:7(709)

678 Huang, S.H., Chen, D.H., 2009. Rapid removal of heavy metal cations and anions from aqueous
679 solutions by an amino-functionalized magnetic-adsorbent. J. Hazard. Mater. 163, 174-179.
680 http://dx.doi.org/10.1016/j.jhazmat.2008.06.075

681 Illès, E., Tombacz, E., 2004. The role of variable surface charge and surface complexation in the
682 adsorption of humic acid on magnetite. Colloids Surf., A 230, 99-109.
683 http://dx.doi.org/10.1016/j.colsurfa.2003.09.017

684 Illés, E., Tombacz, E., 2006. The effect of humic acid adsorption on pH-dependent surface
685 charging and aggregation of magnetite nanoparticles. J. Colloid Interface Sci. 295, 115-123.
686 http://dx.doi.org/10.1016/j.jcis.2005.08.003

687 Jarbling, M., Gunneriusson, L., Hussmann, B., Forsling, W., 2005. Surface complex
688 characteristics of synthetic maghemite and hematite in aqueous suspensions. J. Colloid Interface
689 Sci. 285, 212-217. http://dx.doi.org/10.1016/j.jcis.2004.11.005
690
691 Jolstera, R., Gunneriusson, L., Holmgren, A., 2012. Surface complexation modeling of Fe_3O_4–H^+
692 and magnesium (II) sorption onto maghemite and magnetite. J. Colloid Interface Sci. 386, 260-
693 267. http://dx.doi.org/10.1016/j.jcis.2012.07.031
694

695 Joo, S.H., Zhao, D., 2017. Environmental dynamics of metal oxide nanoparticles in
696 heterogeneous systems: a review. J. Hazard. Mater. 322, 29-47.
697 http://dx.doi.org/10.1016/j.jhazmat.2016.02.068

698 Ju-Nam, Y, Lead, J.R., 2008. Manufactured nanoparticles: An overview of their chemistry,
699 interactions and potential environmental implications. Sci. Total Environ. 400, 396-414.
700 http://dx.doi.org/10.1016/j.scitotenv.2008.06.042

701 Kah, M., 2015. Nanopesticides and nanofertilizers: emerging contaminants or opportunities for
702 rick mitigation? Front. Chem. 64, 1-6. http://dx.doi.org/10.3389/fchem.2015.00064

703 Kakavandi, B., Kalantary, R.R., Jafari, A.J., Nasseri, S., Ameri, A., Esrafili, A., Azari, A., 2015.
704 Pb(II) Adsorption Onto a Magnetic Composite of Activated Carbon and Superparamagnetic
705 Fe_3O_4 Nanoparticles: Experimental and Modeling Study. CLEAN, Soil, Air, Water 43, 1157-
706 1166. http://dx.doi.org/10.1002/clen.201400568

707 Karami, H., 2013. Heavy metal removal from water by magnetite nanorods. Chem. Eng. J. 219,
708 209-216. http://dx.doi.org/10.1016/j.cej.2013.01.022

709 Karimi, Z., Karimi, L., Shokrollahi, H., 2013. Nano-magnetic particles used in biomedicine: Core
710 and coating materials. Mater. Sci. Eng., C 33, 2465–2475.
711 http://dx.doi.org/10.1016/j.msec.2013.01.045

712 Khalafalla, S.E., Reimers, G.W., 1980. Preparation of dilution-stable aqueous magnetic fluids.
713 IEEE Trans. Magn. 16(2), 178-183. http://dx.doi.org/10.1109/TMAG.1980.1060578
714
715 Khot, L.R., Sankaran, S., Maja J.M., Ehsani, R., Schuster, E.W., 2012. Applications of
716 nanomaterials in agricultural production and crop protection: a review. Crop Prot. 35, 64-70.
717 http://dx.doi.org/10.1016/j.cropro.2012.01.007

718 Koesnarpadi, S., Santosa, S.J., Siswanta, D., Rusdiarso, B., 2015. Synthesis and characterization
719 of magnetite nanoparticles coated humic acid (Fe_3O_4/HA). Procedia Environ. Sci. 30, 103-108.
720 http://dx.doi.org/10.1016/j.proenv.2015.10.018

721 Komadel, P., Stucki, J.W., 1988. Quantitative assay of minerals for Fe^{2+} and Fe^{3+} using 1,10-
722 phenantroline: III. a rapid photochemical method . Clays Clay Miner. 36 (4), 379-381.
723 DOI:10.1346/CCMN.1988.0360415

724 Komy, Z.R., Shaker, A.M., Heggy, S.E.M., El-Sayed, M.E.A., 2014. Kinetic study for copper
725 adsorption onto soil minerals in the absence and presence of humic acid. Chemosphere 99, 117-
726 124. http://dx.doi.org/10.1016/j.chemosphere.2013.10.048

Kostic, I., Andelkovic,T., Nikolic, R., Bojic, A., Purenovic, M., Blagojevic S., Andelkovic, D., 2011. Copper(II) and lead (II) complexation by humic acid and humic-like ligands. J. Serb. Chem. Soc. 76 (9), 1325-1336. http://dx.doi.org/10.2298/JSC110310115K

Le, Q.C., Ropers, M.H., Terrisse, H., Humbert, B., 2014. Interactions between phospholipids and titanium dioxide particles. Colloids Surf., B 123, 150-157. http://dx.doi.org/10.1016/j.colsurfb.2014.09.010

Li, J., Hu, J., Ma, C., Wang, Y., Wu, C., Huang, J., Xing, B., 2016. Uptake, translocation and physiological effects of magnetic iron oxide (ɣ-Fe_2O_3) nanoparticles in corn (*Zea mays* L.). Chemosphere 159, 326-334. http://dx.doi.org/10.1016/j.chemosphere.2016.05.083

Li, C.L., Ji, F., Wang, S., Zhang, J.J., Gao, Q., Wu, J.G., Zhao, L.P., Wang, L.C., Zheng, L.R., 2015. Adsorption of Cu(II) on humic acids derived from different organic materials. J. Integr. Agric. 14(1), 168-177. https://doi.org/10.1016/S2095-3119(13)60682-6

Lin, J., Zhan, Y., Zhu, Z., 2011. Adsorption characteristics of Copper (II) ions from aqueous solution onto humic acid-immobilized surfactant-modified zeolite. Colloids Surf., A 384, 9-16. http://dx.doi.org/10.1016/j.colsurfa.2011.02.044

Liu, J.F., Zhao, Z.S., Jiang, G.B., 2008. Coating Fe_3O_4 nanoparticles with humic acid for high efficient removal of heavy metals in water. Environ. Sci. Technol. 42, 6949-6954. http://dx.doi.org/10.1021/es800924c

Liu, J., Arguete, D.M., Murayama, M., Hochella Jr., M., 2009. Influence of size and aggregation on the reactivity of an environmentally and industrially relevant nanomaterial (PbS). Environ. Sci. Technol. 43, 8178-8183. http://dx.doi.org/10.1021/es902121r

Lohdia, J., Mandarano, G., Ferris, N.J., Eu, P., Cowell, S.F., 2010. Development and use of iron oxide (Part 1): synthesis of iron oxide for MRI. Biomed. Imaging Intervention J. 6 (2), 1-11. http://dx.doi.org/10.2349/biij.6.2.e12

Löhr, S.C., Murphy, D.T., Nothdurft, L.D., Bohlar, R., Piazolo, S., Siegel, C., 2017. Maghemite soil nodules reveal the impact of fire on mineralogical and geochemical differentiation at the Earth's surface. Geochim. Cosmochim. Acta 200, 25-41. http://dx.doi.org/10.1016/j.gca.2016.12.011

Lu, A.H., Salabas, E.L., Schuth, F., 2007. Magnetic Nanoparticles: Synthesis, Protection, Functionalization, and Application. Angew. Chem. Int. Ed. 46, 1222 -1244. http://dx.doi.org/10.1002/anie.200602866

Lucas, I., Durand-Vidal, S., Dubois, E., Chevalet, J., Turq, P., 2007. Surface Charge Density of Maghemite Nanoparticles: Role of Electrostatics in the Proton Exchange. J. Phys. Chem. C 111, 18568-18576. http://dx.doi.org/10.1021/jp0743119

761 Madden, A.S., Hochella Jr, M.F., Luxon, T.P., 2006. Insights for size-dependent reactivity of
762 hematite nanomineral surfaces through Cu^{2+} sorption. Geochim. Cosmochim. Acta 70, 4095-
763 4104. http://dx.doi.org/10.1016/j.gca.2006.06.1366

764 Maity, D., Agrawal, D.C., 2007. Synthesis of iron oxide nanoparticles under oxidizing
765 environment and their stabilization in aqueous and non-aqueous media. J. Magn. Magn. Mater.
766 308, 46-55. http://dx.doi.org/10.1016/j.jmmm.2006.05.001

767 Mamindy-Pajany, Y., Hurel, C., Marmier, N., Roméo, M., 2011. Arsenic (V) adsorption from
768 aqueous solution onto goethite, hematite, magnetite and zero-valent iron: Effects of pH,
769 concentration and reversibility. Desalination 281, 93-99.
770 http://dx.doi.org/10.1016/j.desal.2011.07.046

771 Massart, R., 1981. Preparation of aqueous magnetic liquids in alkaline and acidic media.
772 IEEE Trans. Magn. 17, 1247-1248. http://dx.doi.org/10.1109/TMAG.1981.1061188

773 Melcrová, A., Pokorna, S., Pullanchery, S., Kohagen, M., Jurkiewicz, P., Hof, M., Jungwirth, P.,
774 Cremer, P.S., Cwiklik, L., 2016.The complex nature of cation interaction with phospholipid
775 bilayers. Sci. Rep. 38035 (6), 1-12. http://dx.doi.org/10.1038/srep38035

776 Missana, T., Alonso, U., Scheinost, A.C., Granizo, N., Garcia-Gutierrez, M., 2009. Selenite
777 retention by nanocrystalline magnetite: role of adsorption, reduction and dissolution/co-
778 precipitation processes. Geochim. Cosmochim. Acta 73, 6205-6217.
779 http://dx.doi.org/10.1016/j.gca.2009.07.005

780 Mohan, D., Pittman Jr., C.U., Steele, P.H., 2006. Single, binary and multi-component adsorption
781 of copper and cadmium from aqueous solution on kraft-lignin – a biosorbent. J. Colloid Interface
782 Sci. 297, 489-504. https://doi.org/10.1016/j.jcis.2005.11.023

783 Mudunkotuwa, I.A., Grassian, V.H., 2011.The devil is in the details (or the surface): impact of
784 surface structure and surface energetics on understanding the behavior of nanomaterials in the
785 environment. J. Environ. Monit. 13, 1135-1144. http://dx.doi.org/10.1039/c1em00002k

786 Mulder, W.J., Strijkers, G.J., van Tilborg, G.A.F., Griffioen, A.W., Nicolay, K., 2006.
787 Lipid-based nanoparticles for contrast-enhanced MRI and molecular imaging**.** NMR Biomed. 19,
788 142-164. http://dx.doi.org/10.1002/nbm.1011

789 Niu, H., Zhang, D., Zhang, S., Zhang, X., Meng, Z., Cai, Y., 2011. Humic acid coated Fe_3O_4
790 magnetic nanoparticles as highly efficient Fenton-like catalyst for complete mineralization of
791 sulfathiazole. J. Hazard. Mater. 190, 559-565. http://dx.doi.org/10.1016/j.jhazmat.2011.03.086

792 Nowack, B., Bucheli, T.D., 2007. Occurrence, behavior and effects of nanoparticles in the
793 environment. Environ. Pollut. 150, 5-22.
794 http://dx.doi.org/10.1016/j.envpol.2007.06.006

795 Otero-Farina, A., Gago, R., Antelo, J., Fiol, S., Arce, F., 2015. Surface complexation modelling
796 of Arsenic and Copper Immobilization by Iron oxide precipitates derived from Acid Mine
797 Drainage. Boletin de la Sociedad Geologica Mexicana 67, 493-508.
798 http://dx.doi.org/10.18268/BSGM2015v67n3a12

799 Pan, B., Qiu, H., Pan, B., Nie, G., Xiaio, L., Lv, L., Zhang, W., Zhang, Q., Zheng, S., 2010.
800 Highly efficient removal of heavy metals by polymer-supported nanosized hydrated Fe(III)
801 oxides: behavior and XPS study. Water Res. 44, 815-824.
802 http://dx.doi.org/10.1016/j.watres.2009.10.027

803 Pang, S.C., Chin, S.F., Anderson, M.A., 2007. Redox equilibria of iron oxides in aqueous-based
804 magnetite dispersions: Effect of pH and redox potential. J. Colloid Interface Sci. 311, 94-101.
805 http://dx.doi.org/10.1016/j.jcis.2007.02.058

806 Panneerselvam, P., Morad, N., Aik Tan, K., 2011. Magnetic nanoparticle (Fe_3O_4) impregnated
807 onto tea waste for the removal of nickel(II) from aqueous solution. J. Hazard. Mater. 186, 160-
808 168. https://doi.org/10.1016/j.jhazmat.2010.10.102

809 Parkinson, G.S., 2016. Iron oxides surfaces. Surf. Sci. Rep., 71(1), 272-365.
810 https://doi.org/10.1016/j.surfrep.2016.02.001

811 Pédrot, M., Boudec, A.L., Davranche, M., Dia, A., Henin, O., 2011. How does organic matter
812 constrain the nature, size and availability of Fe nanoparticles for biological reduction? J. Colloid
813 Interface Sci. 359, 75-85. http://dx.doi.org/10.1016/j.jcis.2011.03.067

814 Peng, L., Qin, P., Lei, M., Zeng, Q., Song, H., Yang, J., Shao, J., Liao, B., Gu, J., 2012.
815 Modifying Fe_3O_4 nanoparticles with Humic acids for removal of Rhodamine B in water. J.
816 Hazard. Mater. 209-210, 193-198. http://dx.doi.org/10.1016/j.jhazmat.2012.01.011

817 Peng, H., Pearce, C.I., N'Diaye, A.T., Zhu, Z., Ni, J., Rosso, K.M., Liu, J., 2019. Redistribution
818 of electron equivalents between magnetite and aqueous Fe^{2+} induced by a Model Quinone
819 Compound (AQDS). Environ. Sci. Technol. 53 (4), 1863-1873.
820 https://doi.org/10.1021/acs.est.8b05098

821 Peng, H., Pearce, C.I., Huang, W., Zhu, Z., N'Diaye, A.T., Rosso, K.M., Liu, J., 2018. Reversible
822 Fe(II) uptake/release by magnetite nanoparticles. Environ. Sci. Nano, 5, 1545-1555.
823 http://dx.doi.org/10.1039/C8EN00328A

824 Sabbatini, P., Yrazu, F., Rossi, F., Thern, G., Marajofsky, A., Fidalgo de Cortalezzi, M.M., 2010.
825 Fabrication and characterization of iron oxide ceramic membranes for arsenic removal. Water
826 Res. 44, 5702-5712. https://doi.org/10.1016/j.watres.2010.05.059

827 Scherer, C., Neto, A.M.F., 2005. Ferrofluids: properties and applications. Braz. J. Phys. 35 (3A),
828 718-727. http://dx.doi.org/10.1590/S0103-97332005000400018

Schwaminger, S.P., Bauer, D., Fraga-García, P., Wagner, F.E., Berensmeier, S., 2017. Oxidation of magnetite nanoparticles: impact on surface and crystal properties. CrystEngComm. 19, 246-255. http://dx.doi.org/10.1039/c6ce02421a

Senesi, N., Sposito, G., Martin, J.P., 1986. Copper and iron complexation by soil humic acids: an IR and ESR study. Sci. Total Environ. 55, 351-362. https://doi.org/10.1016/0048-9697(86)90192-0

Shaker, MA., Albishri, H.M., 2014. Dynamics and thermodynamics of toxic metals adsorption onto soil-extracted humic acid. Chemosphere 111, 587-595. http://dx.doi.org/10.1016/j.chemosphere.2014.04.088

Sheng, G., Li, J., Shao, D., Hu, J., Chen, C., Chen, Y., Wang, X., 2010. Adsorption of copper(II) on multiwalled carbon nanotubes in the absence and presence of humic or fulvic acids. J. Hazard. Mater. 178, 333-340. https://doi.org/10.1016/j.jhazmat.2010.01.084

Shinoda, W., 2016. Permeability across lipid membranes. Biochim. Biophys. Acta, Biophys. Incl. Photsynth. 1858, 2254-2265. http://dx.doi.org/10.1016/j.bbamem.2016.03.032

Sigg, L., Behra, P., Stumm, W., 2011. Aquatic chemistry, 5th edition, 391pp.

Smith, K.S., 1999. Metal sorption on mineral surfaces: an overview with examples relating to mineral deposits. Reviews in Economic Geology, 6A-6B, Chapter 7, 161-182.

Solis-Calero, C., Ortega-Castro, J., Frau, J., Munoz, F., 2015. Non-enzymatic reactions above phospholipid surfaces of biological membranes: reactivity of phospholipids and their oxidation derivatives. Oxid. Med. Cell. Longevity 15, 1-22. http://dx.doi.org/10.1155/2015/319505

Stumm, W., 1992. Chemistry of the Solid-Water interface. Processes at the Mineral-Water and Particle-Water interface in natural systems. Wiley-VCH, 448pp. ISBN: 978-0-471-57672-3.

Tang, S.C.N., Lo, I.M.C., 2013. Magnetic nanoparticles: Essential factors for sustainable environmental applications. Water Res. 47, 2613-2632. http://dx.doi.org/10.1016/j.watres.2013.02.039

Tang, W.W., Zeng, G.M., Gong, J.L., Liang, J., Xu, P., Zhang, C., Huang, B.B., 2014. Impact of Humic/fulvic acid on the removal of heavy metals from aqueous solutions using nanomaterials: A review. Sci. Total Environ. 468-469, 1014-1027. http://dx.doi.org/10.1016/j.scitotenv.2013.09.044

Tipping, E., 2002. Cation binding to humic substances. Cambridge University Press, 2002. https://doi.org/10.1017/CBO9780511535598

Tombacz, E., Toth, I.Y., Nesztor, D., Illés, E., Hadju, A., Szekeres, M., Vékas, L., 2013. Adsorption of organics on magnetite nanoparticles, pH dependent stability and salt tolerance. Colloids Surf., A 435, 91-96. http://dx.doi.org/10.1016/j.colsurfa.2013.01.023

Vatta, L.L., Sanderson, R.D., Koch, K.R., 2006. Magnetic nanoparticles: properties and potential applications. Pure Appl. Chem. 78, 1793-1801. https://doi.org/10.1351/pac200678091793

Vindedahl, A.M., Strehlau, J.H., Arnold, W.A., Penn, R.L., 2016. Organic matter and iron oxide nanoparticles: aggregation, interactions and reactivity. Environ. Sci. Nano, Critical Review 3, 494-505. http://dx.doi.org/10.1039/c5en00215j

Wang, L., Li, J., Jiang, Q., Zhao, L., 2012. Water-soluble Fe_3O_4 nanoparticles with high solubility for removal of heavy-metal ions from waste water. Dalton Trans. 41, 4544-4551. http://dx.doi.org/10.1039/c2dt11827k

Wu, W., Wu, Z., Yu, T., Jiang, C., Kim, W.S., 2015. Recent progress on magnetic iron oxide nanoparticles: synthesis, surface functional strategies and biomedical applications. Sci. Technol. Adv. Mater. 16, 023501 – 023544. http://dx.doi.org/10.1088/1468-6996/16/2/023501

Xu, P., Zheng, G., Huang, D., Lai, C., Zhao, M., Wei, Z., Li, N., Huang, C., Xie, G., 2012. Adsorption of Pb(II) by iron oxide nanoparticles immobilized Phanerochaete chrysosporium: Equilibrium, kinetic, thermodynamic and mechanisms analysis. Chem. Eng. J. 203, 423-431. http://dx.doi.org/10.1016/j.cej.2012.07.048

Ye, S., Zheng, G., Wu, H., Zhang C., Dai, J., Liang, J., Yu, J., Ren, X., Yi, H., Cheng, M., Zhang, M., 2017. Biological technologies for the remediation of co-contaminated soil. Crit. Rev. Biotechnol. 37(8), 1062-1076. https://doi.org/10.1080/07388551.2017.1304357

Yéghicheyan, D., Bossy, C., Bouhnik Le Coz, M., Douchet, C., Granier, G., Heimburger, A., Lacan, F., Lanzanova, A., Rousseau, T.C.C., Seidel, J.L., Tharaud, M., Candaudap, F., Chmeleff, J., Cloquet, C., Delpoux, S., Labatut, M., Losno, R., Pradoux, C., Sivry, Y., Sonke, J.E., 2013. A compilation of silicon, rare earth element and twenty-one other trace element concentrations in the natural river water reference material slrs-5 (nrc-cnrc). Geostand. Geoanal. Res. 37(4), 449-467. https://doi.org/10.1111/j.1751-908X.2013.00232.x

Yu, S., Liu, J., Yin, Y., Shen, M., 2018. Interactions between engineered nanoparticles and dissolved organic matter: a review on mechanisms and environmental effects. J. Environ. Sci. 63, 198-217. http://dx.doi.org/10.1016/j.jes.2017.06.021

Zasonska, B.A., Bober, P., Jostr, P., Eduard, P., Bostık, P., Horak, D., 2016. Magnetoconductive maghemite core/polyaniline shell nanoparticles: Physico-chemical and biological assessment. Colloids Surf., B 14, 382-389. http://dx.doi.org/10.1016/j.colsurfb.2016.01.059

Zhang, Y., Chen, Y., Westerhoff, P., Crittenden, J., 2009. Impact of natural organic matter and divalent cations on the stability of aqueous nanoparticles. Water Res. 43, 4249-4257. http://dx.doi.org/10.1016/j.watres.2009.06.005

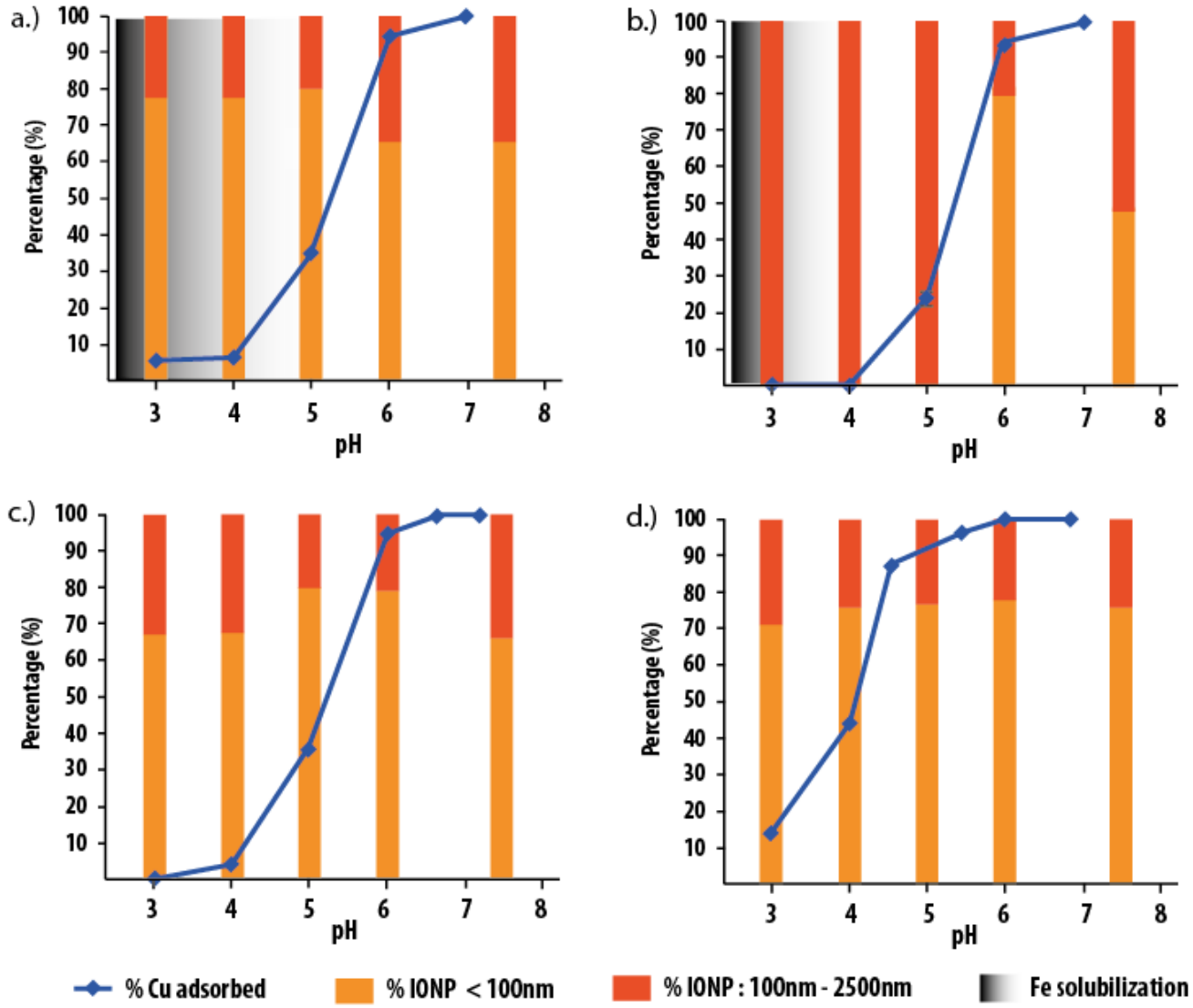

Figure 1: Adsorbed Cu%, aggregates sizes and Fe dissolution versus pH on the four IONP: (a) magnNP, (b) maghNP, (c) PC-magnNP and (d) HA-magnNP. The data were obtained at the same initial NP concentration (NP= 0.5 g L^{-1}), ionic strength = 5 10^{-3} M NaCl, and starting Cu = 0.05 mM. The error bars, resulting from triplicates, are within the markers. The intensity of IONP dissolution is represented by dark areas (black to light grey refer to high to decreased dissolution rate).

Table 1: Fe concentrations (mg L^{-1}) released from the IONP relative to the pH (from triplicates). The experiments were conducted at 0.5 g L^{-1} IONP suspensions with a constant ionic strength of 5.10^{-3} M NaCl. LQ refers to the Fe limit of quantification (0.12 µg L^{-1}).

	pH 3	pH 4	pH 5	pH 6	pH 7
MagnNP	5.23 ± 0.08	1.34 ± 0.07	0.005 ± 0.001	<LQ	<LQ
MaghNP	1.63 ± 0.07	0.33 ± 0.05	<LQ	<LQ	<LQ
PC-magnNP	0.009 ± 0.001	0.001 ± 0.001	<LQ	<LQ	<LQ
HA-magnNP	0.006 ± 0.001	0.0007 ± 0.001	<LQ	<LQ	<LQ